Core-level shifts in fcc random alloys: A first-principles approach

W. Olovsson,[1] C. Göransson,[2] L. V. Pourovskii,[3] B. Johansson,[1,4] and I. A. Abrikosov[2]
[1]*Condensed Matter Theory Group, Department of Physics, Uppsala University, SE-751 21 Uppsala, Sweden*
[2]*Department of Physics and Measurement Technology, Linköping University, SE-581 83 Linköping, Sweden*
[3]*Department of Theoretical Physics, University of Nijmegen, Nijmegen 6500 GL, The Netherlands*
[4]*Applied Materials Physics, Department of Materials Science and Engineering, Royal Institute of Technology, SE-100 44 Stockholm, Sweden*

(Received 22 February 2005; revised manuscript received 21 June 2005; published 8 August 2005)

First-principles theoretical calculations of the core-level binding-energy shift (CLS) for eight binary face-centered-cubic (fcc) disordered alloys, CuPd, AgPd, CuNi, NiPd, CuAu, PdAu, CuPt, and NiPt, are carried out within density-functional theory (DFT) using the coherent potential approximation. The shifts of the Cu and Ni $2p_{3/2}$, Ag and Pd $3d_{5/2}$, and Pt and Au $4f_{7/2}$ core levels are calculated according to the complete screening picture, which includes both initial-state (core-electron energy eigenvalue) and final-state (core-hole screening) effects in the same scheme. The results are compared with available experimental data, and the agreement is shown to be good. The CLSs are analyzed in terms of initial- and final-state effects. We also compare the complete screening picture with the CLS obtained by the transition-state method, and find very good agreement between these two alternative approaches for the calculations within the DFT. In addition the sensitivity of the CLS to relativistic and magnetic effects is studied.

DOI: 10.1103/PhysRevB.72.064203 PACS number(s): 71.15.−m, 71.23.−k, 79.60.Ht

I. INTRODUCTION

A binding energy of a spectral line for a core electron of an atom A in an alloy $A_{1-x}B_x$ is in general different from the binding energy of the corresponding line in the pure metal A, which gives rise to the so-called core-level binding-energy shift (CLS). The shift is sensitive to differences in the chemical environment of the atom, and by studying the CLS one can gain a deeper understanding of the underlying physical properties, the bonding, and the electronic structure of a solid. It is relatively easy to measure binding energies by means of x-ray photoelectron spectroscopy (XPS), and the CLS is often referred to as the chemical shift when given by the electron spectroscopy for chemical analysis (ESCA), developed by Siegbahn and co-workers[1] in the 1960s. It is worth noting that the development led to the Noble prize awarded in 1981.

There are different kinds of binding-energy shifts that have been studied over the years. For instance one studies shifts between free atoms and the atoms in a metal, as well as shifts between an atom in the bulk and at the surface, the so-called surface CLS (SCLS). Among the different properties which have been related to the CLS are cohesive energies,[2] heats of mixing,[3,4] segregation energies,[5] and charge transfer.[6–8] The experimental spectra can be used to determine what elements are present in a sample. Further, a comparison with calculated shifts can, for instance, help to determine the structure of a sample.[9]

Core-level shifts have been experimentally determined for various alloys. In experiments the binding energy $E_B > 0$ and the measured CLS (chemical shift) in alloys is defined as

$$E_{CLS}^{exp} = E_B^{A_{1-x}B_x} - E_B^A. \quad (1)$$

In a classical paper by Steiner and Hüfner[4] the experimental core-level shifts of eight binary alloy systems, namely AgPd, CuNi, CuAu, NiPd, CuZr, PdZr, and PdTi, are presented. The CuPd alloys were studied experimentally in Ref. 3. Unfortunately it is often the case that the exact degree of ordering of the alloys is not discussed in the experimental papers. But it is known that AgPd, CuNi, CuAu, NiPd, and CuPd are all fcc disordered alloys over the whole concentration interval at some temperatures above the order-disorder transition temperatures.

Also, there are many theoretical studies devoted to the CLS problem. Already in the beginning binding-energy shifts were linked to differences in the on-site atomic potentials ΔV within the ESCA potential model.[6] In particular, this "potential model" was applied to molecular systems, where shifts may be as large as 5 eV.[6] In solids, however, they are typically small, usually less than 1 eV. Though the potential model was used for the interpretation of the experimental results for CuPd alloys,[7,8] a consistent quantitative approach seems to call for a more elaborate treatment.

To get a more accurate description of the CLS there are a variety of contributing factors which need to be taken into account. Possible effects are listed by Weinert and Watson.[10] They mention changes in the screening of the final-state core hole, changes in the reference level (the Fermi level), intra-atomic charge transfer (between electrons of *sp* and *d* state), and a redistribution of charge due to bonding and hybridization, in addition to the interatomic charge transfer. It would be difficult to treat all these effects simultaneously on a model level. On the other hand, one can perform first-principle calculations in the framework of the density-functional theory (DFT). Unfortunately, the calculations in the case of alloys seem to be quite demanding, and in the literature relatively few theoretical shifts are reported. Moreover, one is often forced to do simple estimations of the CLS within the so-called initial-state model, where one calculates shifts of the Kohn-Sham eigenvalues between an atom in the pure metal and in the alloy. For example, CLSs in fcc CuPd,

AgPd, and CuZn systems were recently investigated within the initial-state approach.[11]

While the initial state contribution comes from the energy eigenvalues of a particular core electron before ionization, there are also the final-state effects, which consist of the energy relaxation due to the screening of the core hole left behind the core-electron ionization. The initial- and final-state shifts are in principle two nonmeasurable quantities, but they are invaluable as a tool to describe the observed binding-energy shifts. The importance of the final-state effects for the core-level *shifts* is mostly due to the possible differences in the effective screening of a core hole in a metal and in an alloy by electrons that may have different orbital characters, i.e., *sp* and *d*, as *d* electrons are in general more tightly bound. As a matter of fact, it is possible to study changes of the screening of the core holes created in the photoemission process with concentration experimentally by means of the so-called Auger parameter.[12]

One possible way to determine *ab initio* CLS that includes the initial-, as well as the final-, state effects is suggested within the model which uses the Slater-Janak transition rule applied to DFT.[13] This approach has recently been used for calculation of various kinds of shifts, the CLS in adlayers on surfaces,[14] the Mg 1*s* and Au 4*f* shifts in fcc disordered AuMg alloy,[15] and also x-ray fluorescence shift.[16] Within this model one again uses the eigenstates of the Kohn-Sham Hamiltonian for the analysis of the CLS, but varies the occupation number of a particular core level at one atom in a system, and in doing so one accounts for the screening of the core hole.

On the other hand, the core-level binding energies in Eq. (1) are essentially differences between the total energies of a solid in its unperturbed initial state and in the final state, that contains a single core-ionized atom. This means that in principle the core-level shift can be obtained from differences in total energies. For a review see, for example, Ref. 17. In the present work the CLS was calculated according to the complete screening picture, suggested by Johansson and Mårtensson,[2] which is essentially based on this idea. An advantage with the complete screening picture is that both initial-state and final-state effects are directly included in the same computational scheme.

The complete screening picture was originally used in a successful thermodynamic model approach, which connects the initial and final states of the core ionization by means of a Born-Haber cycle. Here a core-ionized atom Z^* is substituted with an atom of atomic number $Z+1$, leading to an essentially similar screening from the valence electrons. Therefore the model is usually called the $(Z+1)$-or the quasiatomic model. In particular, it was used in this way to calculate the core-level shift between a free atom and an atom in a metal.[2] One can also employ the complete screening picture together with *ab initio* methods. This was done, for example, in order to calculate the CLS at surfaces (SCLS),[9,18,19] with good results. For the case of CLS in random alloys the complete screening picture was used by us in a recent work for the disordered fcc CuPd and AgPd alloys, and it was shown that the final-state effects cannot be neglected in these cases.[20,21] Here we want to show that one can consistently perform accurate first-principle calculations of the CLS in random alloys in the framework of DFT using the complete screening picture. The CLS are calculated *ab initio* for eight different disordered fcc alloys CuPd, AgPd, CuNi, NiPd, CuAu, PdAu, CuPt, and NiPt over the whole composition range for each system. For the total-energy calculations of random alloys we use the numerically efficient coherent potential approximation (CPA).

We elucidate on the importance of the final-state effects and make a direct comparison between the results obtained by the complete screening picture, by the transition-state method, and within the initial-state approach. Also, we investigate the importance of including the spin-orbit coupling term directly, as well as the influence of magnetic contribution on the CLS in ferromagnetic alloys.

II. METHODOLOGY

A. The complete screening picture

The main assumption of the complete screening picture is that the symmetric part of the measured core line directly corresponds to a state in which the conduction electrons are fully relaxed in the presence of a core hole. Therefore within the complete screening picture one basically compares the differences in a kind of "ionization" energies E_I for the excitation of an electron situated at a particular core level in atom A, into the conduction band. The CLS is then given by

$$E_{CLS}^{th} = E_I^{A_{1-x}B_x} - E_I^A. \tag{2}$$

Note that this directly corresponds to the procedure in which the experimental shift is obtained in Eq. (1).

Each ionization energy E_I in Eq. (2) represents a difference between the energy of a system with a core electron excited on a single atom, and the energy of an original, unperturbed, system. In other words, it can be calculated in exactly the same way, as the impurity solution energy, where the core ionized atoms are treated as impurities in the host metal or alloy. The latter can be calculated in different ways[18,19,22,23] and in the present work it is obtained from the generalized thermodynamic chemical potential (GTCP),[20] which is given by

$$\mu = \left.\frac{\partial E_{tot}}{\partial c}\right|_{c\to 0}. \tag{3}$$

Here E_{tot} represents the total energy of a completely random alloy $A_{1-x}B_x$ (or a metal A), in which a particular core electron on some A atoms has been promoted to the conduction band, with the concentration c of the core ionized atoms A in the alloy (metal). In this work the concentrations of ionized atoms in the system ranged from $c=0-2\,\%$. The chemical potential is calculated in practice by an extrapolation to zero concentration c. The CLS will then be given by the difference between the GTCPs in the pure metal and in the alloy,

$$E_{CLS}^{cs} = \mu_{alloy} - \mu_{pure}. \tag{4}$$

It is worth noticing that the total energy of a system, E_{tot}, which is the basis for the complete screening picture, is typically the most reliable quantity given by DFT. Note that the energies of the systems with core ionized atoms, i.e., for-

mally excited states, in practice also represent the DFT ground-state energies within the complete screening picture. It is also possible to generalize the complete screening picture to calculate the Auger kinetic energy shift,[24] which was recently done *ab initio* for the LMM Auger transitions in AgPd alloys, with excellent agreement with experiment.[25]

As was already mentioned in the introduction, one can easily carry out independent calculations of the initial-state shifts, by comparing the core electron energy eigenvalues, relative to the Fermi energy, of an atom in the metal and in the alloy,

$$E_{CLS}^{is} = \{E_F^{A_{1-x}B_x} - \varepsilon_i^{A_{1-x}B_x}\} - \{E_F^A - \varepsilon_i^A\}, \tag{5}$$

where ε_i are the eigenvalues for a certain core level i of the atom A in the metal and in the alloy $A_{1-x}B_x$, respectively, and E_F are the Fermi energies of the corresponding systems. Note that the sign convention is chosen in agreement with experimental definition of the CLS, Eq. (1). The resulting initial-state shift E_{CLS}^{is}, may be used to provide an estimate of the final-state effects, from its comparison to the CLS obtained by the complete screening picture, $E_{CLS}^{cs} - E_{CLS}^{is} = -\Delta E_R$, following the convention in the ESCA potential model. We will show that the complete screening picture is in general more accurate, as compared to the initial-state model. We will also show that in many cases the relaxation energies ΔE_R are not small.

B. Slater-Janak transition-state model

In 1978 Janak developed an extension of DFT by introducing occupation numbers for the Kohn-Sham orbitals in the equation for the charge density:[13]

$$n(\mathbf{r}) = \sum_i \eta_i |\psi_i(\mathbf{r})|^2, \tag{6}$$

where η_i are occupation numbers ($0 \leqslant \eta_i \leqslant 1$). By using η_i it is possible to solve a set of modified Kohn-Sham equations self-consistently, even for nonintegral values of the occupation numbers. The introduction of the occupation numbers yields a modified kinetic-energy functional, $\tilde{T}$ which in turn gives a total-energy functional $\tilde{E}$. In general $\tilde{E} \neq E$, but if η_i have the form of Fermi-Dirac distribution, $\tilde{E}$ is numerically equal to E. The so-called *Janak's theorem* states that

$$\frac{\partial \tilde{E}}{\partial \eta_i} = \varepsilon_i, \tag{7}$$

independently of the form of the exchange-correlation functional.[13] It follows from Eq. (7) that when η_i have the form of a Fermi-Dirac distribution, $\tilde{E}$ is minimized at the end points (η_i is equal to 1 or 0) and then, as mentioned above, it is equal to the ground-state energy of the system.

Carrying out an integration of Eq. (7) makes it possible to connect the ground states of the N- and $(N+1)$-particle systems, by inserting η electrons into the lowest unoccupied level:[13]

$$E_{N+1} - E_N = \int_0^1 \varepsilon_i(\eta_i) d\eta_i. \tag{8}$$

This integral can be identified as the binding energy $-E_i$ for the top-most valence electron. If the one-electron eigenenergy ε_i depends *linearly* upon the occupation number η_i, the integral in Eq. (8) can be written

$$E_{N+1} - E_N \approx \varepsilon_i(1/2) \approx \varepsilon_i(0) + \frac{1}{2}[\varepsilon_i(1) - \varepsilon_i(0)], \tag{9}$$

where the last equation separates the initial- and final-state contributions. The first equality in Eq. (9) gives a useful tool to calculate the binding energy for an electron and it is known as the Slater-Janak transition state. However, the last equality is more physically appealing since it separates the initial- and final-state contributions. The evaluation "at midpoint" can be carried out numerically relatively easily by assuming that the particular core state is just half occupied. In order to retain charge neutrality of the system, we increase correspondingly the occupation number for valence electrons by the same half an electron.

Equation (9) provides us with a way to calculate the CLS. By relating the core-level eigenvalues to the Fermi level, the following formula for calculating the CLS within the transition state model can be applied,

$$E_{CLS}^{ts} = \{E_F^{A_{1-x}B_x} - \varepsilon_i^{A_{1-x}B_x}(1/2)\} - \{E_F^A - \varepsilon_i^A(1/2)\}. \tag{10}$$

Notice the similarity to the scheme of calculating the initial-state shift in Eq. (5). The transition-state model of calculating shifts is common in the literature, see, for instance Refs. 14, 15, and 26, and it gives a good agreement with experiment. Over the past years there has been an ongoing discussion concerning the validity of Janak's theorem.[27] Though being an important discussion, we do not comment on it in this paper. Rather, we seek to compare the complete screening pictures with the transition-state method and initial-state calculations as tools for obtaining the core level shifts.

C. Computational details

To calculate all the total energies of the various systems involved in the derivation of the GTCPs in Eq. (3) and core electron energy eigenvalues needed for the transition-state model Eq. (10) and the initial-state shift Eq. (5), we use the density-functional theory (DFT).[28,29] The electronic structure problem is solved using the Green's-function technique within the atomic sphere approximation (ASA).[30–34] We use equal atomic sphere radii for both alloy components, as well as for core ionized atoms. Our basis set includes *spdf* orbitals. The disorder problem is treated within the coherent potential approximation (CPA).[33–35] As was shown in Ref. 22, the CPA is particularly well suited for the calculations of the partial molar quantities, like the GTCP in Eq. (3). The fully relativistic extension of the code has been developed[36] using a $\{\kappa\mu\}$ basis set and the linear muffin-tin orbital (LMTO) technique for relativistic non-spin-polarized systems, proposed by Godreche and others.[37–39]

Within the complete screening picture, self-consistent iterations were carried out using the local-density approxima-

TABLE I. Parameters of the screened impurity model α and β, Eqs. (11) and (12) used in the CPA calculations for the random fcc alloys.

Alloy	AgPd	NiPd	CuPd	CuPt	CuNi	CuAu	PdAu	NiPt
α	0.72	0.75	0.81	0.79	0.72	0.76	0.68	0.76
β	1.10	1.17	1.20	1.16	1.10	1.16	1.10	1.14

tion (LDA) for the exchange-correlation contribution to the one-electron potential. The calculated charge density was used as an input for the total-energy calculations where the general gradient approximation (GGA) was applied. Our tests show that this procedure leads to results equivalent to those obtained by a consistent use of the GGA, but is more stable numerically due to somewhat better convergence within the LDA. Note that for the calculations within the transition-state model, as well as for fully relativistic calculations, GGA was used also for the self-consistent calculations. GGA, as well as LDA exchange-correlation functions, were parametrized according to Perdew *et al.*.[40]

Notice that in the earlier studies,[20,21] a basis set of *spd* orbitals and the LDA were used. Moreover, we now include multipole corrections to the ASA within the so-called ASA $+M$ method,[34,41] and take the charge-fluctuation effects into account using the screened impurity model (SIM),[42–44] with parameters adjusted according to the procedure described in detail in Refs. 45 and 46. For the latter quantities, the calculations are first carried out for 256 atoms in the supercell that mimics an equiatomic random alloy at a volume close to the theoretical equilibrium volume. For the supercell calculations we employ the locally self-consistent Green's-function method (LSGF).[47,48] Within the LSGF method the contribution due to charge fluctuations to the Madelung potential and energy are determined essentially exactly. Within the SIM-CPA approach, these contributions are given by the following two equations:

$$V_M^i = -\frac{e^2}{2}\langle q_i\rangle\frac{\alpha}{S}, \tag{11}$$

$$E_M = -x(1-x)\beta\frac{e^2}{2}(\langle q_A\rangle - \langle q_B\rangle)^2\frac{\alpha}{S}, \tag{12}$$

where $\langle q_i\rangle$ represents the average net charge at atomic sites A and B and S corresponds to the radius of the Wigner-Seitz sphere. α is the on-site screening constant, while β is the Madelung energy renormalization coefficient. The screening parameters are derived by requiring a consistency between the CPA and the LSGF calculations for each particular system (without the presence of the core-ionized atoms), and the results are listed in Table I. These parameters may depend only weakly on volume and concentration, and in practice the dependence can be safely neglected. In addition, we assume that the parameters do not change for alloys in the presence of core-ionized atoms. To justify this, we compare the CLS results obtained within the complete screening picture by means of LSGF and CPA for selected alloys. In agreement with our earlier assessments,[20] we see that the difference is very small. The largest difference found was below 0.1 eV. This should be compared with the experimental accuracy, which is typically of the order of 0.1 eV.

The lattice parameters of all the investigated systems, metals and alloys, with and without core-ionized atoms, were chosen as to minimize total energies of corresponding systems, rather than to represent experimental values. This provides an accurate and consistent theoretical treatment of the problem. Local lattice relaxation effects are not included in the present study. In principle this factor can have an effect on the alloy total energies when atoms in the alloy have very different sizes. However, in our experience the influence of the local lattice relaxations on the CLS does not seem to be of crucial importance, judging from the very good agreement of our calculated results with experiment, as will be shown below. In any case, we would like to emphasize that the goal of the present work is to investigate the trends for CLS over the whole composition range and for a large number of alloys. For the same reason, the theory assumes a completely random distribution of alloy components in the systems, that is we neglect any short-range order that may be present in practice. In addition, we calculate the CLS representative for the solid bulk region, while the experimental results are sometimes affected by a contribution from the surface. A sensitivity of the CLS to the local environment effects, including the lattice relaxation, will be presented elsewhere.

III. RESULTS AND DISCUSSION

The core-level shifts calculated within the complete screening picture in the fcc random alloys AgPd, NiPd, CuPd, CuPt, CuNi, CuAu, PdAu, and NiPt are presented and discussed along four different lines to provide a clear overview. First in Sec. III A, a direct comparison is made between the theoretical shifts and experimental data available in the literature for the studied alloys. Next in Sec. III B the calculated CLSs are analyzed in terms of the initial- and final-state effects. In Sec. III C a comparison is made between the complete screening picture and the transition-state method. In the final Sec. III D we discuss contributions from the spin-orbit coupling to the CLS within the fully relativistic approach. Also, the sensitivity of the CLS to magnetic ordering is studied in the case of the CuNi, NiPd, and NiPt alloys.

A. Core-level shifts by the complete screening picture: Comparison with the experiment

The CLSs calculated according to the complete screening picture are displayed in Fig. 1. The CLS in these systems were studied experimentally in many works,[3,4,49–59] and we include the experimental results in Fig. 1. According to the

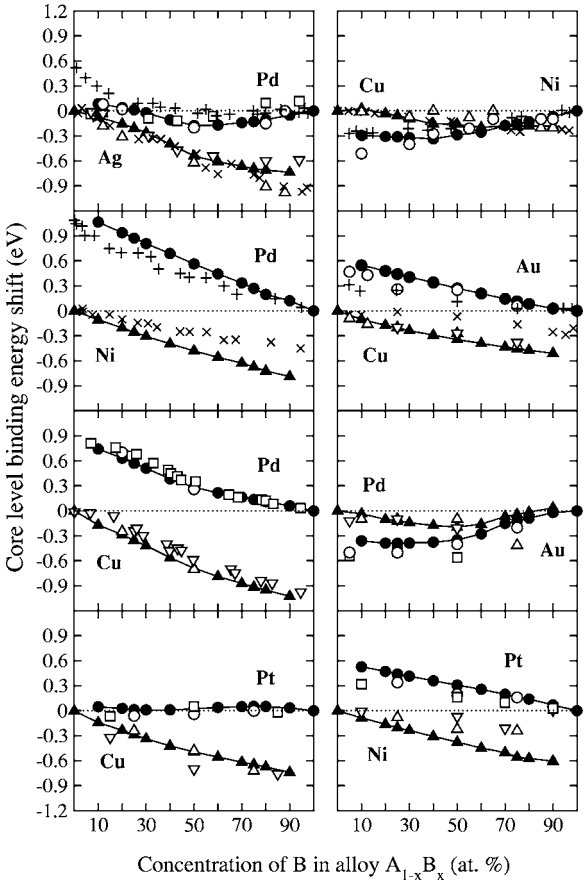

FIG. 1. Core-level shifts calculated by the complete screening picture (filled symbols, fully drawn lines) are compared to experimental values (unfilled symbols) for the fcc disordered alloys $A_{1-x}B_x$: on the left-hand side, from top to bottom, are CLSs in AgPd, NiPd, CuPd, and CuPt, and on the right-hand side; CuNi, CuAu, PdAu, and NiPt. The experimental results from Steiner and Hüfner (Ref. 4) are denoted by $\times$ (component A) and $+$ (B), for the AgPd, NiPd, CuNi, and CuAu alloys. Other experimental values are grouped together using pairwise the symbols triangle up and circle ($\triangle$ $\bigcirc$), and second, triangle down and box ($\triangledown$, $\square$). Apart from Ref. 4 experimental values were taken from: AgPd (Refs. 49 and 50), CuPd (Refs. 3 and 51), CuPt (Refs. 51 and 52), CuNi (Ref. 49), CuAu (Refs. 53 and 54), PdAu (Refs. 55 and 56), and finally NiPt (Refs. 51 and 57).

phase diagrams disordered fcc alloys are stable over the whole concentration interval for all the investigated alloys at sufficiently high temperatures.[60] Unfortunately, the degree of short-range order is not always clearly determined in the experimental studies. In our calculations the fcc alloys are assumed to be completely random. The ordering may influence CLS, but this will be the subject for a separate study. Starting with the left panel of Fig. 1, from top to bottom, we show the result for the AgPd, NiPd, CuPd, and CuPt binding-energy shifts of Ag and Pd $3d_{5/2}$, as well as Ni and Cu $2p_{3/2}$ and Pt $4f_{7/2}$ core levels, as a function of the atomic concentration of the component B in $A_{1-x}B_x$ alloys. The right-hand side of the figure, from top to bottom, displays the results for the CuNi, CuAu, PdAu, and NiPt alloys, with the shifts of Cu and Ni $2p_{3/2}$, Pd $3d_{5/2}$, Au and Pt $4f_{7/2}$ core levels as a function of at. % B. See caption of Fig. 1 for further details. The choice of the particular core state for each element is determined by the experimental information available in the literature. The theoretical CLS for CuNi, NiPd, and NiPt is here calculated assuming the ferromagnetic order in the alloys, which corresponds to the magnetic ground state of the Ni-rich alloys at ambient temperature, i.e., at the conditions used for the measurement of CLSs.

Starting with the shifts in the AgPd system, the displayed experimental data are taken from Steiner and Hüfner[4] and more recent works.[49,50] We first note the change in sign for the Pd $3d$ CLS, positive for low concentrations of Pd to negative and around zero at 30 at. % Pd. While Ref. 4 gives a large Pd CLS, about 0.5 eV, in the very low Pd concentration region, this is not seen in the other experiments. In fact, Barbieri *et al.*[49] point out that this is due to different experimental preparations, namely the use of thin-film alloys in Ref. 4. Notice that the complete screening picture reproduces the recent experimental data[49,50] very well for Pd. Considering the Ag shift, the experimental values decrease essentially linearly from zero towards −0.9 eV at high Pd concentrations. Also here the theory agrees well with the experiment, though the theory seems to underestimate the shift in the low Ag concentration limit, compared to Refs. 4 and 50.

Turning to the NiPd and CuPd alloys it is of interest to note the similarities and differences in their calculated and experimental binding-energy shifts. Studying the E_{CLS}^{cs} of Ni and Cu, they both show a nearly linear decrease with Pd concentration from zero towards −0.6 and −0.9 eV, in the respective alloys. The experimental values are taken from Ref. 4 for NiPd, and Refs. 3 and 51 in the case of CuPd. In comparison with experiment the agreement is excellent for Cu $2p$ CLS, even at low Cu concentrations. The Ni $2p$ shift is increasingly overestimated with theory predicting about 0.3 eV more negative shift at high Pd concentrations, which in fact is the largest deviation from experiment in the present study. At the same time, the calculated CLS of Pd $3d$ follows the experimental results very well over the whole concentration interval in both the CuPd and NiPd alloys. One notices that while the concentration dependence is almost linear in NiPd, it is slightly more curved in CuPd. However, the changes are not so dramatic, e.g., no changes of signs, as in the case of AgPd alloy.

For the CuPt system the theoretical shifts agree very well with the experimental values.[51,52] The Pt $4f$ shift is near zero over the whole composition interval, which is closely reproduced by the complete screening picture. Discussing the theoretical trend for Pt CLS, one can notice a small curving, similar to that of Pd in AgPd, while Cu $2p$ appears to follow a linear behavior towards −0.7 eV.

Continuing the comparison between E_{CLS}^{cs} and experiment, we turn to the alloys in the right panel of Fig. 1, starting with CuNi. In the CuNi system one notices that the experimental $2p$ core-level shifts for Cu and Ni atoms[4,49] are both negative, or zero, over the whole concentration interval, with a reasonably good agreement between theory and experiment. The concentration dependencies of the shifts are not linear. For both Cu- and Ni-rich alloys the shift on the solvent is about −0.2 eV,[4] though the most recent experiment gives a larger shift at Ni in $Cu_{90}Ni_{10}$, about −0.55 eV.[49]

In the CuAu alloys E_{CLS}^{cs} depend linearly on the concentration, approaching the absolute value of 0.6 eV, with opposite signs, in the low concentration limit for both Au 4*f* and Cu 2*p* components. Comparing different experimental sources, one notices the difference between data from Steiner and Hüfner[4] which give shifts of both Au 4*f* and Cu 2*p* closer to zero and with a different curvature, than the values from Refs. 53 and 54. The theoretical shifts agree very well with the later experiments. As was pointed out in the case of AgPd,[49] an origin of the difference between different experiments could be associated with surface effects, because in Ref. 4 the experiment was carried out for thin films.

Turning to the calculated CLS in PdAu alloys, one immediately recognize the similarity of the Pd 3*d* shift with the case of AgPd. While the calculations follow the experiment[55,56] closely for Au 4*f* shift, there is a larger difference in the trend for Pd in the low Pd concentration limit, e.g., at 75 at. % Au.[55] The final comparison between experiment and theory is for the NiPt alloys. Here experiments are taken from Refs. 51 and 57. The theoretical Pt 4*f* shift is good, while Ni 2*p* gives a worse result with an almost linear dependence on concentration towards −0.6 eV in the low Ni concentration limit. This result for Ni 2*p* seems to be in line with what was found for it on the NiPd alloy and the experimental ambiguity for the low Ni concentration limit in CuNi.

Summarizing the above comparison between the CLS obtained within the complete screening picture and from the experiment, we would like to notice that they are in very good agreement. In general, the difference between theory and experiment is of the order of 0.1 eV, with the exception of the Ni 2*p* shift in NiPd and NiPt alloys. This corresponds to the experimental accuracy for the determination of the CLS, and is sometimes smaller than the spread between different sets of experimental data.

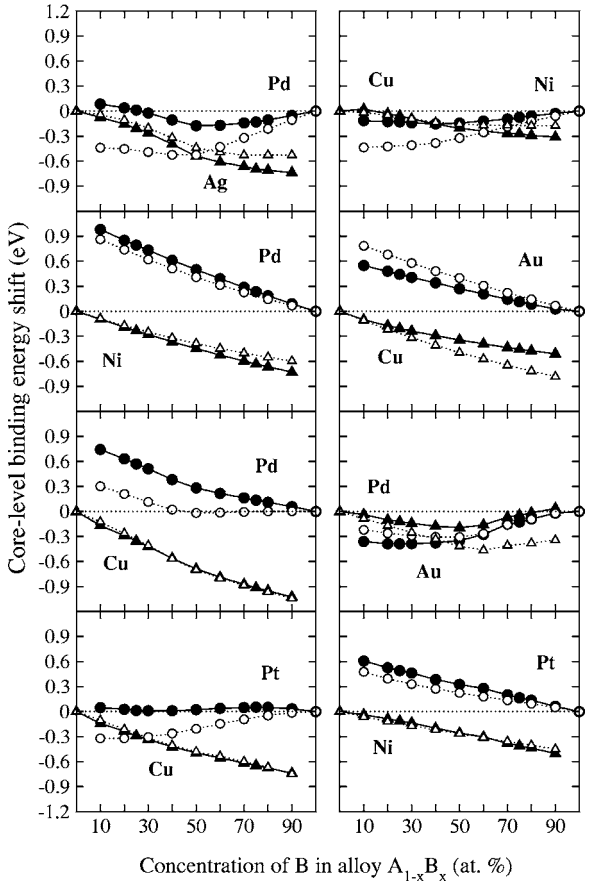

FIG. 2. CLSs calculated by the complete screening picture (filled symbols, fully drawn lines) are compared to the initial-state shifts (open symbols, dotted lines) for the eight fcc disordered alloys. The arrangement of graphs and the symbols are the same as in Fig. 1.

B. Influence of final-state effects

To understand the origin of the binding-energy shifts in solids or at surfaces, it is important to answer the question of how the final-state effects influence the easily estimated initial-state shifts in metals. Also, though the basic idea of the complete screening picture is to include both the initial- and final-state effects in the same self-consistent scheme, we still would like to investigate and explain our theoretical results according to the initial- and final-state contributions. In the present section such a study is made for all the investigated alloys, and the complete screening shifts E_{CLS}^{cs} from Eq. (4) are compared to the initial-state shifts E_{CLS}^{is}, Eq. (5), in Fig. 2. The arrangement of the graphs is the same as in Fig. 1. Both E_{CLS}^{cs} and E_{CLS}^{is} in Fig. 2 refer to nonmagnetic ordering in all the alloys and Ni metal, in contrast to Fig. 1 and the previous section, where the calculations are done for ferromagnetic ordering in CuNi, NiPd, NiPt, as well as in Ni.

From Fig. 2 one can conclude that in general the initial-state model represents a reasonable estimate of the CLS. There are, however, important exceptions. For example, starting with the AgPd system, one notices that the behavior of the Pd 3*d* CLS is very much determined by an increasingly larger contribution from final-state effects. It grows from pure Pd to about 40 at. % Pd, keeping the total CLS around zero. At lower Pd concentrations the final-state contribution becomes nearly constant. The Ag 3*d* shift on the other hand shows a smaller dependence on final-state effects, which are still not entirely negligible, especially for the Pd-rich alloys. These effects have been noticed earlier,[20] where they were explained in terms of a change in the orbital character of the screening charge, from *d* in Pd-rich alloy to gradually more *sp*, in Ag-rich alloys.

To elaborate on this point, let us now turn to the CLS in three other alloys, which contain Pd; NiPd, CuPd, and AuPd. While the concentration dependence of the Pd CLS in NiPd and CuPd alloys are quite similar to each other, a closer inspection of the initial-state contribution to the total CLS shown in Fig. 2 shows that the influence of the final-state effects differs a lot in these two cases. For the Pd CLS in the NiPd alloy, there are only small final-state effects, which slightly adjust the results for Pd in a more positive direction. On the contrary, the Pd CLS in the CuPd alloys are more akin to the situation encountered in the isoelectronic AgPd alloy. The Pd 3*d* initial-state shift is almost zero when proceeding from pure Pd to 40 at. % Pd concentration, where it increases to 0.25 eV in an alloy with 10 at. % Pd. Notice that

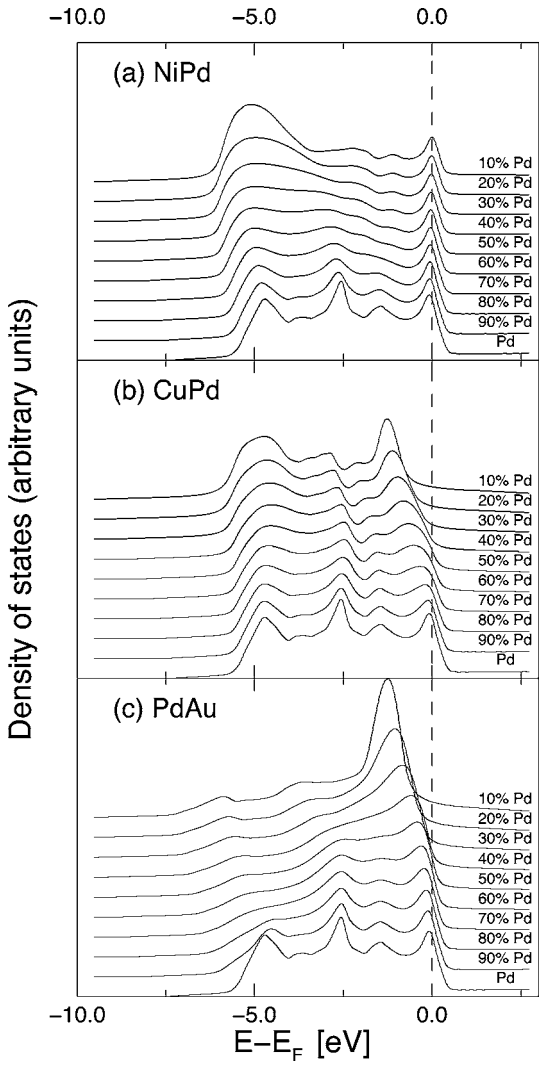

FIG. 3. The restricted average local density of states at Pd in (a) NiPd, (b) CuPd, and (c) PdAu fcc random alloys with different concentrations as a function of energy (relative to the Fermi energy E_F).

even the magnitude of the final-state effects to a large degree is the same as for Pd in AgPd. In PdAu the situation is similar to the one found in AgPd and CuPd, namely that there is a substantial contribution to the CLS from the final-state effects. As a matter of fact, the Pd 3*d* total and initial-state shift behave as in AgPd, with a somewhat smaller magnitude of E^{is}_{CLS}. We note in passing that for Ni and Au atoms in NiPd and PdAu alloys the final-state effects are smaller compared to those for Ag in AgPd alloys. The Cu 2*p* CLS shows virtually no final-state effects, even going to high Pd concentrations.

From the analysis above, we conclude that the magnitude of the final-state contribution to the CLS for the *same* atom, Pd, is different in different alloys, indicating the importance of the electronic structure effects. To further discuss the behavior of the Pd CLS, the corresponding restricted average local density of states (DOS) for Pd is plotted for NiPd, CuPd, and PdAu alloys in Figs. 3(a)–3(c), respectively. By comparing DOS at the Fermi level and slightly above, i.e., looking at the electronic states that contribute to the screening of the core hole, one notices the similarity between pure Pd and Pd in the NiPd alloys, while for CuPd there is a clear change of the orbital character of the unoccupied states at E_F from predominantly *d* to *sp* type in alloys with decreasing Pd concentration, a trend similar to the case of AgPd.[20] Investigating the valence-band DOS of Pd in PdAu, Fig. 3(c), a situation very similar to CuPd is found, with a marked change in the screening charge as a function of concentration. This is so because Ni and Pd are isoelectronic elements. Though they belong to different *d* series, 3*d* and 4*d*, respectively, and therefore have different bandwidths, as well as there exists substantial charge-transfer effects in the NiPd alloys, this is not sufficient to fill the Pd *d* band, and change the orbital character of the screening charge. On the contrary, in alloys of Pd with noble metals, which have fully occupied *d* bands shifted away from the Fermi level, the Pd *d* band becomes occupied, and the screening electrons must occupy *sp* states in alloys with low (roughly less than 50 at. %) Pd composition.

Turning to the CuPt systems, the final-state effect on Cu 2*p* is indeed very small, similar to the result in CuPd. On the contrary there is a pronounced effect for Pt 4*f*, and it is clearly seen that the final-state effect is responsible for the almost zero total core-level shift. Notice the similarity to the trend for Pd 3*d* in AgPd. For the CuNi alloys, there is a small but noticeable difference between the initial-state shift and that of the complete screening picture, especially if one compares to the situation in CuPt. Interestingly the final-state effect is quite substantial for the nonmagnetic Ni case, and is particularly large in the Cu-rich alloys. Similar to the case of Pd, this can be explained by the change of the orbital character of the screening charge due to a formation of the so-called virtual bound state at Ni,[35,61] which is shifted away from the Fermi level towards lower energies.

In CuAu there seems to be a noticeable contribution from the final-state effects on both components over the whole range of alloy compositions. Interestingly this cannot be immediately explained by a direct study of the unoccupied states close to the Fermi level,[62] as was done for the other alloys, though we remark that the inclusion of final-state effects clearly improve the agreement with the recent experiments. We will return to this problem in the discussion of the transition-state model. Finally going to the NiPt alloys, there is large similarity between the trends, both as regards the complete screening picture CLS and the final-state effects, to the NiPd system; namely virtually no final-state effect for Ni and a small effect for the Pd and Pt components. The result is in accordance with what was found in the case of the isoelectronic NiPd alloys.

Summarizing this section, we can suggest a very simple recipe for the applicability of the initial-state model, often employed for the calculations of the CLS in the literature. We conclude that in principle the CLS could be estimated via much simpler calculations of the initial-state shifts combined with the analysis of the unoccupied part of the valence-band DOS just above the Fermi energy. The reliability of the initial-state results can be justified if there is no change of the orbital character of the latter between the system of interest

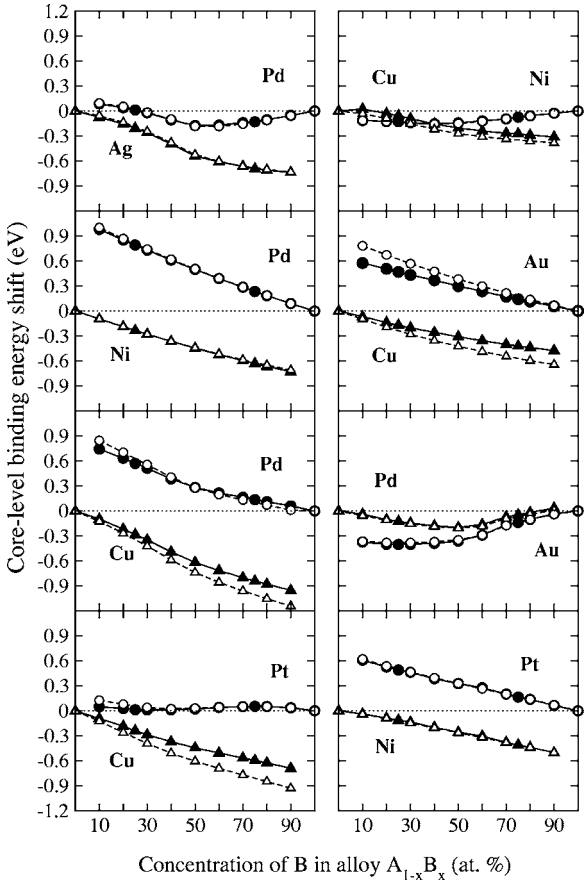

FIG. 4. CLS calculated from the complete screening picture (filled symbols, fully drawn lines) are compared to the corresponding CLS given by the transition-state method (open symbols, dashed lines).

and the reference system. Obviously, this is not true for all the alloys in the present study.

C. Complete screening picture and the transition-state model

In this section a comparison is made between the complete screening picture and the transition-state model for calculating core-level shifts in alloys (see Fig. 4). Here all the results are for nonmagnetic CuNi, NiPd, and NiPt alloys, and the reference Ni metal.

One immediately notices that the shifts obtained from the two different methods are quite similar. The agreement is remarkable, given the very different physical picture behind the two models, with the underlying density-functional theory as the only point in common. Still, there is a good correspondence between both the trends and the absolute values of the calculated CLS, though with some interesting exceptions. While E_{CLS}^{ts} almost exactly reproduce the result of E_{CLS}^{cs} over the whole composition range for the NiPd, NiPt, and PdAu alloys, there is a difference towards a larger negative shift for Cu $2p$, which grows in the low Cu concentration limit, most pronounced in CuAu and CuPt alloys. The results for Ni $2p$ are here virtually identical between the two different methods. Also worth noting are the differences in the very low concentration limit for Pd in AgPd and CuPd. CuAu is the only system among the investigated alloys that shows a substantial difference between the transition-state model and the complete screening picture for both atomic components. Interestingly E_{CLS}^{ts} reproduce the initial-state results for CuAu in Fig. 2, though the former include the final-state effects, while the latter do not. We have already pointed out in the previous section that an investigation of the valence-band density of states[62] do not immediately support the fact that the final-state contribution to the CLS should be large in CuAu. Good agreement between the transition-state and initial-state results may derive from the fact that the final-state contribution to the CLS is indeed small in CuAu, in contrast to the conclusion drawn from the complete screening calculations. This issue requires further investigation because CuAu alloys is, as a matter of fact, the only case where our calculations do not lead to a consistent picture.

D. Influence of relativistic and magnetic effects

Here we will discuss the core-level shift obtained within the complete screening picture by fully relativistic calculations for the AgPd and PdAu alloys. Also, the CLS calculated for nonmagnetic and ferromagnetic alloys containing Ni, namely NiPd, NiPt, and CuNi, will be discussed. This allows us to investigate the influence of the spin-orbit cou-

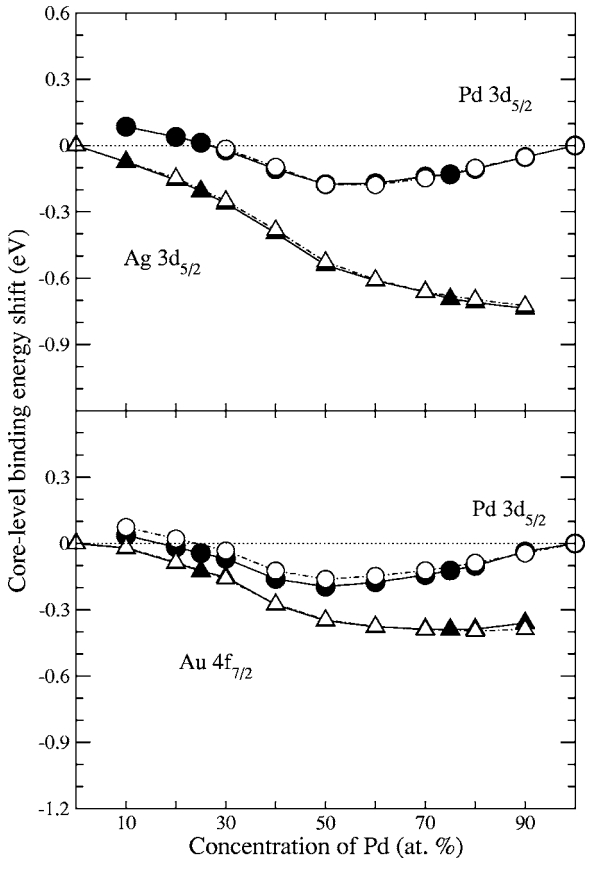

FIG. 5. Core-level shifts calculated using the fully relativistic (open symbols, dot-dashed lines) and the scalar relativistic (filled symbols, full lines) approaches are shown. Calculations are done for two alloys, AgPd and PdAu. All calculations are done according to the complete screening picture.

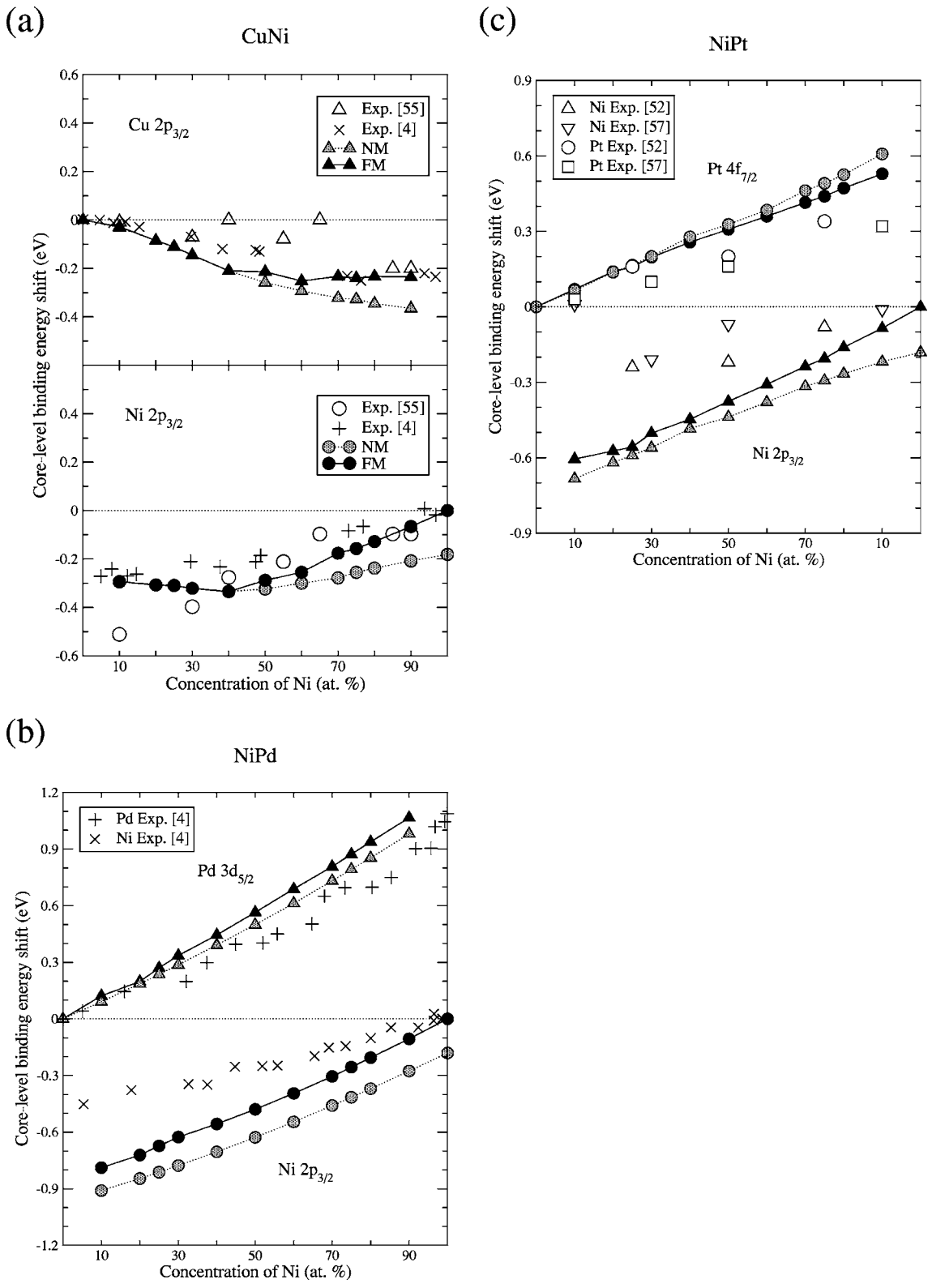

FIG. 6. Core-level shifts are shown for (a) Cu and Ni $2p_{3/2}$ levels in fcc disordered CuNi alloy. Nonmagnetic (NM, shaded symbols, dotted lines) results are compared to the result of the ferromagnetic calculations (FM, full symbols, drawn lines) and experimental values (open symbols). The CLS are calculated within the complete screening picture. (b) The corresponding results for Ni $2p_{3/2}$ and Pd $3d_{5/2}$ in NiPd alloy. (c) The results for Ni $2p_{3/2}$ and Pt $4f_{7/2}$ in NiPt alloy. For the CLS at Ni, the FM Ni is chosen as a reference in all cases.

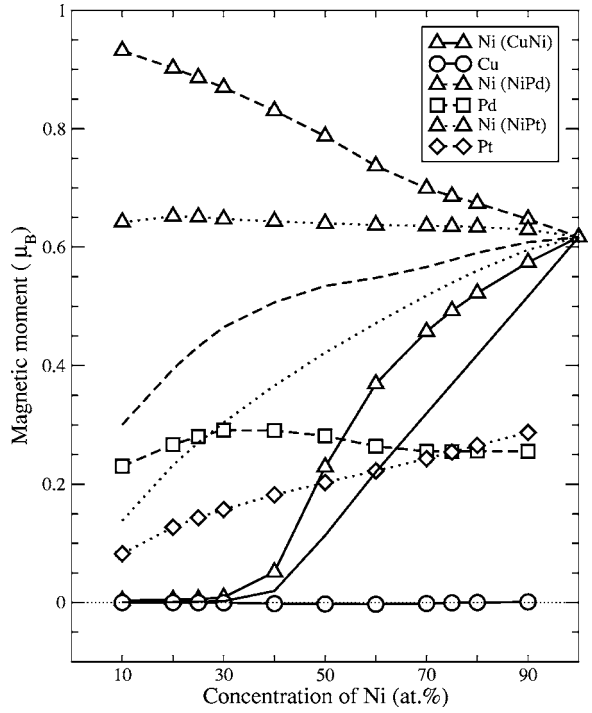

FIG. 7. The magnetic moment per atom in CuNi (full lines), NiPd (dashed lines), and NiPt (dotted lines) alloys are plotted as a function of Ni concentration. Local moments on Ni sites are shown by triangles, on Cu by circles, on Pd by squares, and on Pt by diamonds. Lines without symbols show net magnetic moments in alloys.

pling and the effects due to magnetism on the resulting CLS.

Let us start with relativistic effects. In the upper panel of Fig. 5 are the $3d_{5/2}$ CLSs on Ag and Pd, while in the bottom panel are the $3d_{5/2}$ CLS of Pd, $4f_{7/2}$ CLS of Au, as a function of Pd concentration. For both the AgPd and PdAu alloys we see that the effect from the inclusion of the spin-orbit coupling is negligible, despite the fact that the atoms are relatively heavy. A detailed scalar relativistic study of the CLS in the AgPd alloy was previously presented by some of us in Ref. 20. The results and conclusions of this study therefore are not affected by the neglect of the spin-orbit coupling. We would like to note that fully relativistic calculations were also done for CuPd, CuPt, and CuAu alloys at selected compositions. The overall conclusion is that though there could be an effect due to the neglect of the spin-orbit coupling in the scalar-relativistic calculations, it is in general quite small or vanishing, compared to the magnitude of the shift in the studied systems.

Next, let us investigate the influence of magnetic order on CLS in Ni-based alloys. Note that though they are prepared at high temperatures to keep the systems in a chemically disordered state, CLS measurements are most often taken on quenched samples at room temperature, and therefore one can expect the presence of ferromagnetic ordering in the samples.

The core-level shift for ferromagnetic and nonmagnetic CuNi, NiPd, and NiPt is displayed in Figs. 6(a)–6(c). Only scalar relativistic calculations were carried out. The calculated magnetic moments from these three alloys are shown in Fig. 7. They are in very good agreement with experiment for CuNi (Ref. 63) and NiPd (Ref. 64) systems. The agreement is worse for the NiPt system,[64] where the experimental magnetic moments decrease faster with Pt concentration. A possible reason for this disagreement is the presence of ordered phases in this alloy,[65] in contrast to the CuNi and NiPd systems.

In all three cases we have chosen the reference for the CLS calculations to be ferromagnetic (FM) Ni. Pure Pd, Pt, and Cu are considered nonmagnetic, which leads to the −0.18-eV nonmagnetic (NM) shift at 100% Ni concentration. Starting with NiPd in Fig. 6(b) the calculations give a clear difference between the two magnetic configurations, with a ~0.15-eV more positive shift for FM, consistently over the whole composition range. Of course, if we refer the NM shift to NM Ni, the two sets of calculations, the FM and NM would almost coincide. A very similar behavior is observed in NiPt, Fig. 6(c), though in this case the two curves are less parallel than in the NiPd case. Here Pt have a slightly larger CLS in the high Ni concentration for NM calculations, while the opposite trend is seen for Pd in NiPd alloy. But the effect is very small, less than 0.1 eV, and therefore it is unlikely that the experiment can see the difference. Turning to the result for CuNi in Fig. 6(a) it is seen that the different magnetic phases give rise to quite different CLSs. The Ni $2p$ shifts start to differ already at high Ni concentrations, with FM shift being less negative. The calculated NM and FM CLSs in Cu are equal to each other from pure Cu to about 40 at. % Cu, where both the pure Cu and the alloys are nonmagnetic. But for lower concentrations of Cu the FM shift is almost constant, in agreement with experiment, while the NM shift continues to decrease. In this case the effect is as large as 0.2 eV for high Ni concentrations, and it can be seen experimentally. In general, the agreement with the experiment is better for the FM calculations. The sensitivity of the CLS to the magnetic splitting seems to be a general effect. Recently, we also observed it in our study of Pd-Mn surface alloys.[9]

IV. SUMMARY

The core-level binding-energy shifts were calculated within density-functional theory according to the complete screening picture for the eight fcc random alloys, AgPd, NiPd, CuPd, CuNi, CuAu, PdAu, CuPt, and NiPt, over the whole concentration range. We have shown that our approach, based on DFT and the coherent potential approximation, produces good agreement with experimental data. In general, the difference between theory and experiment is at most of the order of 0.1 eV. This corresponds to the experimental accuracy for the determination of the CLS, and is sometimes smaller than the spread between different sets of experimental data. Of course, the calculation scheme can be improved by taken into account such factors as the local lattice relaxations and the ordering effects in the alloys. However, the influence of these effects seems not to be as important for the CLS problem, as it is in some other cases.

We also investigated the importance of the final-state effects, and found that they are not negligible in many cases.

At the same time, we suggest a very simple recipe for testing the applicability of the initial-state model without doing more complex complete screening calculations. Namely, we show that the CLS can be estimated via the initial-state shifts combined with the analysis of the unoccupied part of the valence-band DOS just above the Fermi energy. The reliability of the initial-state results can be justified if there is no change of the orbital character of the latter between the system of interest and the reference system.

We compared the CLS calculated within the complete screening picture with those obtained by the transition-state model, and find very good agreement between the two sets of results. The agreement is remarkable, given the very different physical picture behind the two models, with the only point in common, the underlying density-functional theory. We also find that the fully relativistic treatment, which takes into account the spin-orbit coupling has only a marginal effect on the calculated CLS. At the same time, the shift is sensitive to the magnetic structure of the alloy.

Note that CLS can be used to estimate the heat of formation for substitutional alloys, thus providing a link between electronic structure properties and alloy energetics. The binding-energy shifts can also be used to probe the local chemical environment of an atom. The success of the present study will motivate us to treat other interesting problems, like the disorder broadening of the binding-energy lines in disordered alloys, the CLSs in multilayers and in surface alloys, as well as in other cases.

ACKNOWLEDGMENTS

Useful discussions with Professor A. V. Ruban and Professor P. Weightman are acknowledged. We are grateful to the Swedish Research Council (VR) and the Swedish Foundation for Strategic Research (SSF) for financial support. Part of the calculations were performed on Monolith cluster at the National Supercomputer Centre (NSC) in Linköping, and at the High Performance Computing Center North (HPC2N) in Umeå, Sweden.

[1] K. Siegbahn, C. Nordling, A. Fahlman, R. Nordberg, K. Hamrin, J. Hedman, G. Johansson, T. Bergmark, S-E. Karlsson, I. Lindgren, and B. Lindberg, *ESCA Atomic, Molecular and Solid State Structure Studied by Means of Electron Spectroscopy* (Almqvist & Wiksells, Uppsala, 1967).
[2] B. Johansson and N. Mårtensson, Phys. Rev. B **21**, 4427 (1980).
[3] N. Mårtensson, R. Nyholm, H. Calén, J. Hedman, and B. Johansson, Phys. Rev. B **24**, 1725 (1981).
[4] P. Steiner and S. Hüfner, Acta Metall. **29**, 1885 (1981).
[5] A. Rosengren and B. Johansson, Phys. Rev. B **23**, 3852 (1981).
[6] U. Gelius, Phys. Scr. **9**, 133 (1974).
[7] R. J. Cole, N. J. Brooks, and P. Weightman, Phys. Rev. Lett. **78**, 3777 (1997).
[8] R. J. Cole, N. J. Brooks, and P. Weightman, Phys. Rev. B **56**, 12178 (1997).
[9] W. Olovsson, E. Holmström, A. Sandell, and I. A. Abrikosov, Phys. Rev. B **68**, 045411 (2003).
[10] M. Weinert and R. E. Watson, Phys. Rev. B **51**, 17168 (1995).
[11] J. S. Faulkner, Y. Wang, and G. M. Stocks, Phys. Rev. Lett. **81**, 1905 (1998).
[12] N. D. Lang and A. R. Williams, Phys. Rev. B **20**, 1369 (1979).
[13] J. F. Janak, Phys. Rev. B **18**, 7165 (1978).
[14] M. V. Ganduglia-Pirovano, J. Kudrnovský, and M. Scheffler, Phys. Rev. Lett. **78**, 1807 (1997).
[15] M. Methfessel, V. Fiorentini, and S. Oppo, Phys. Rev. B **61**, 5229 (2000).
[16] J. Lægsgaard, Phys. Rev. B **63**, 193102 (2001).
[17] W. F. Egelhoff, Jr., Surf. Sci. Rep. **6**, 253 (1987).
[18] M. Aldén, H. L. Skriver, and B. Johansson, Phys. Rev. Lett. **71**, 2449 (1993).
[19] M. Aldén, I. A. Abrikosov, B. Johansson, N. M. Rosengaard, and H. L. Skriver, Phys. Rev. B **50**, 5131 (1994).
[20] I. A. Abrikosov, W. Olovsson, and B. Johansson, Phys. Rev. Lett. **87**, 176403 (2001).
[21] W. Olovsson, I. A. Abrikosov, and B. Johansson, J. Electron Spectrosc. Relat. Phenom. **127**, 65 (2002).
[22] A. V. Ruban and H. L. Skriver, Phys. Rev. B **55**, 8801 (1997).
[23] B. Drittler, M. Weinert, R. Zeller, and P. H. Dederichs, Phys. Rev. B **39**, 930 (1989).
[24] N. Mårtensson, P. Hedegård, and B. Johansson, Phys. Scr. **29**, 154 (1984).
[25] W. Olovsson, I. A. Abrikosov, B. Johansson, A. Newton, R. J. Cole, and P. Weightman, Phys. Rev. Lett. **92**, 226406 (2004).
[26] M. Birgersson, C.-O. Almbladh, M. Borg, and J. N. Andersen, Phys. Rev. B **67**, 045402 (2003).
[27] M. M. Valiev and G. W. Fernando, Phys. Rev. B **52**, 10697 (1995).
[28] P. Hohenberg and W. Kohn, Phys. Rev. **136**, B864 (1964).
[29] W. Kohn and L. J. Sham, Phys. Rev. **140**, A1133 (1965).
[30] O. K. Andersen, Phys. Rev. B **12**, 3060 (1975).
[31] O. K. Andersen and O. Jepsen, Phys. Rev. Lett. **53**, 2571 (1984).
[32] H. L. Skriver and N. M. Rosengaard, Phys. Rev. B **43**, 9538 (1991).
[33] I. A. Abrikosov and H. L. Skriver, Phys. Rev. B **47**, 16532 (1993).
[34] A. V. Ruban and H. L. Skriver, Comput. Mater. Sci. **15**, 119 (1999).
[35] J. S. Faulkner, Prog. Mater. Sci. **27**, 1 (1982) for a review.
[36] L. V. Pourovskii, Ph.D. thesis, Uppsala University, 2003.
[37] C. Godreche, J. Magn. Magn. Mater. **29**, 262 (1982).
[38] V. V. Nemoshkalenko, A. E. Krasovski, V. N. Antonov, V. N. Antonov, U. Fleck, H. Wonn, and P. Ziesche, Phys. Status Solidi B **120**, 283 (1984).
[39] N. E. Christensen, Int. J. Quantum Chem. **25**, 233 (1984).
[40] J. P. Perdew, K. Burke, and M. Ernzerhof, Phys. Rev. Lett. **77**, 3865 (1996).
[41] P. A. Korzhavyi, I. A. Abrikosov, B. Johansson, A. V. Ruban, and H. L. Skriver, Phys. Rev. B **59**, 11693 (1999).
[42] I. A. Abrikosov, Yu. H. Vekilov, P. A. Korzhavyi, A. V. Ruban, and L. E. Shilkrot, Solid State Commun. **83**, 867 (1992).

[43] P. A. Korzhavyi, A. V. Ruban, I. A. Abrikosov, and H. L. Skriver, Phys. Rev. B **51**, 5773 (1995).
[44] A. V. Ruban, I. A. Abrikosov, and H. L. Skriver, Phys. Rev. B **51**, 12958 (1995).
[45] A. V. Ruban and H. L. Skriver, Phys. Rev. B **66**, 024201 (2002).
[46] A. V. Ruban, S. I. Simak, P. A. Korzhavyi, and H. L. Skriver, Phys. Rev. B **66**, 024202 (2002).
[47] I. A. Abrikosov, A. M. N. Niklasson, S. I. Simak, B. Johansson, A. V. Ruban, and H. L. Skriver, Phys. Rev. Lett. **76**, 4203 (1996).
[48] I. A. Abrikosov, S. I. Simak, B. Johansson, A. V. Ruban, and H. L. Skriver, Phys. Rev. B **56**, 9319 (1997).
[49] P. F. Barbieri, A. de Siervo, M. F. Carazolle, R. Landers, and G. G. Kleiman, J. Electron Spectrosc. Relat. Phenom. **135**, 113 (2004).
[50] A. W. Newton, S. Haines, P. Weightman, and R. J. Cole, J. Electron Spectrosc. Relat. Phenom. **136**, 235 (2004).
[51] A. W. Newton Ph.D. thesis, University of Liverpool, Liverpool, 2001.
[52] Y.-S. Lee, K.-Y Lim, Y.-D. Chung, C.-N. Whang, and Y. Jeon, Surf. Interface Anal. **30**, 475 (2000).
[53] M. Kuhn and T. K. Sham, Phys. Rev. B **49**, 1647 (1994).
[54] T. K. Sham, A. Hiraya, and M. Watanabe, Phys. Rev. B **55**, 7585 (1997).
[55] P. A. P. Nascente, S. G. C. de Castro, R. Landers, and G. G. Kleiman, Phys. Rev. B **43**, 4659 (1991).
[56] Y.-S. Lee, Y. Jeon, Y.-D. Chung, K.-Y. Lim, C.-N. Whang, and S.-J. Oh, J. Korean Phys. Soc. **37**, 451 (2000).
[57] E. Choi, S.-J. Oh, and M. Choi, Phys. Rev. B **43**, 6360 (1991).
[58] A. W. Newton, A. Vaughan, R. J. Cole, and P. Weightman, J. Electron Spectrosc. Relat. Phenom. **107**, 185 (2000).
[59] S. R. Haines, A. W. Newton, and P. Weightman, J. Electron Spectrosc. Relat. Phenom. **137-40**, 429 (2004).
[60] P. Villars and L. D. Calvert, *Pearson's Handbook of Crystallographic Data for Intermetallic Phases* (American Society for Metals, Metals Park, OH, 1985).
[61] J. S. Faulkner and G. M. Stocks, Phys. Rev. B **21**, 3222 (1980).
[62] The restricted average local density of states at Cu and Au were calculated over the whole concentration interval for fcc random CuAu alloys and compared to the pure metals. No significant changes were found for the unoccupied part near the Fermi level as in the case for Pd in Figs. 3(b) and 3(c).
[63] Ni—Cu, in *Magnetic Properties of Metals*, edited by H. P. J. Wijn, Landolt-Börnstein New Series, Group III, Vol. 19, Pt. b (Springer-Verlag, Berlin, 1987), p. 52.
[64] Ni alloys and compounds, in *Magnetic Properties of Metals*, edited by H. P. J. Wijn, Landolt-Börnstein New Series, Group III, Vol. 19, Pt. a (Springer-Verlag, Berlin, 1986), p. 618.
[65] Co and Ni alloys, in *Magnetic Properties of Metals*, edited by H. P. J. Wijn, Landolt-Börnstein New Series, Group III, Vol. 32, Pt. a (Springer-Verlag, Berlin, 1997), p. 380.